Supplemental material

Williamson and Vale, https://doi.org/10.1083/jcb.201711175

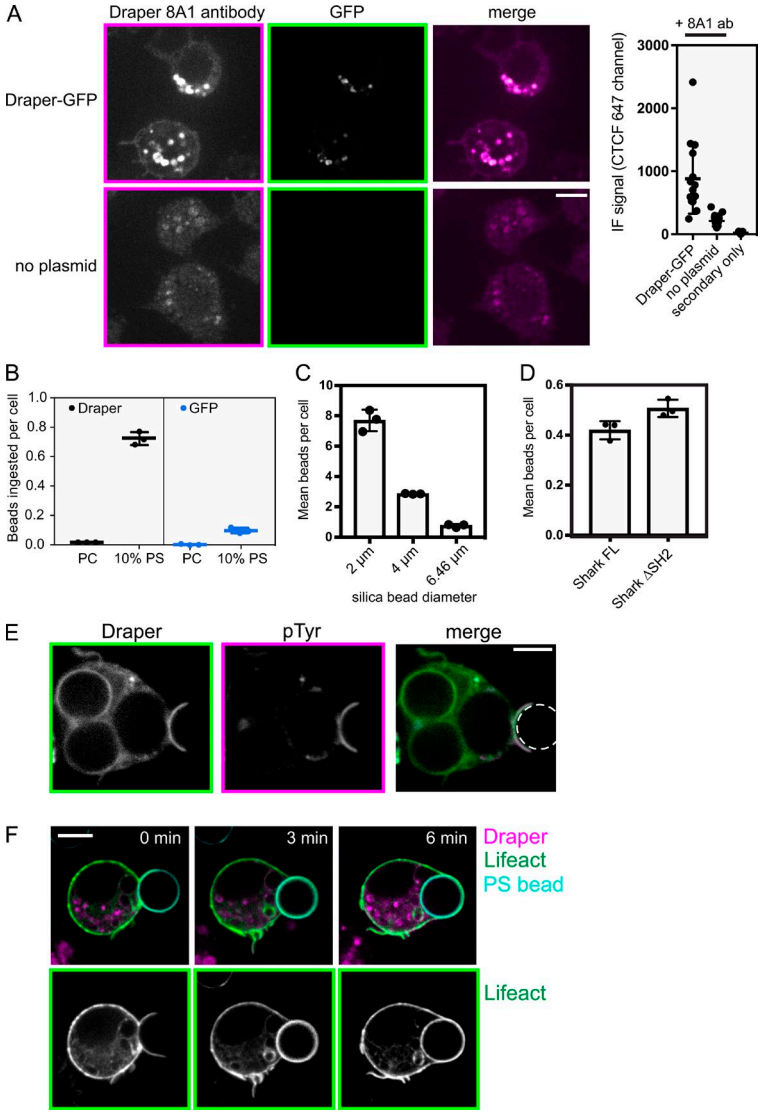

Figure S1. **Characterization of the Draper-GFP S2 system (related to Fig. 1). (A)** Left: Draper-GFP and endogenous Draper show similar subcellular localization. S2 cells transfected with Draper-GFP or no plasmid were stained with the 8A1 anti-Draper antibody. Draper 8A1 antibody stills (left) and GFP (middle) are scaled equally. Right: Draper-GFP is overexpressed approximately fivefold in our system. The mean immunofluorescence (IF) signal is shown as CTCF of the 647 channel (anti-Draper secondary). Draper-GFP: CTCF above secondary background = 860, n = 15; endogenous Draper (no plasmid): CTCF above secondary background = 190; secondary only: CTCF 22, n = 13. CTCF = integrated density – (area of cell × mean background signal for the same image; mean ± SD is plotted for each condition). **(B)** Draper overexpression increases PS bead phagocytic proficiency approximately sevenfold. S2 cells were transfected with either Draper-GFP or a GFP control vector and incubated with PC or 10% PS beads for 30 min at 27°C. The mean number of beads fully ingested per cell for three independent biological replicates are shown (mean ± SD). **(C)** Internalization increases as bead diameter decreases. S2 cells were transfected with Draper-GFP and mCherry-CAAX and incubated with 10% PS beads for 30 min at 27°C. The number of beads fully ingested per cell for three independent biological replicates is shown (mean ± SD). **(D)** Shark-mCherry overexpression does not increase PS-bead internalization. S2 cells were transfected with Draper-GFP and either Shark-mCherry full-length (FL) or Shark ΔSH2-mCherry, a mutant that cannot be recruited to the plasma membrane by Draper-GFP and incubated with 10% PS beads for 30 min at 27°C. The number of beads fully ingested per cell for three independent biological replicates is shown (mean ± SD). **(E)** Draper-GFP is Tyr phosphorylated at the interface with a 10% PS bead. Draper-GFP$^+$ S2 cells were incubated with 10% PS beads. After a 30-min incubation, cells were fixed, permeabilized, and stained with pTyr antibody. pTyr staining is enriched at the synapse between bead and cell. During fixation and permeabilization, the lipid bilayer on the bead is stripped off; bead position is indicated by dashed white line. pTyr signal was enriched at 31 synapses of 31 examined. **(F)** F-actin projections around a PS bead. Upon completion of the phagocytic cup, beads are internalized. Draper-GFP/LifeAct-BFP S2 cells were incubated with 10% PS/0.1% rhodamine-PE beads and imaged every 3 min by spinning-disk confocal microscopy. A middle section from a z stack video is shown. Stills are taken from Video 1. Bars, 5 µm.

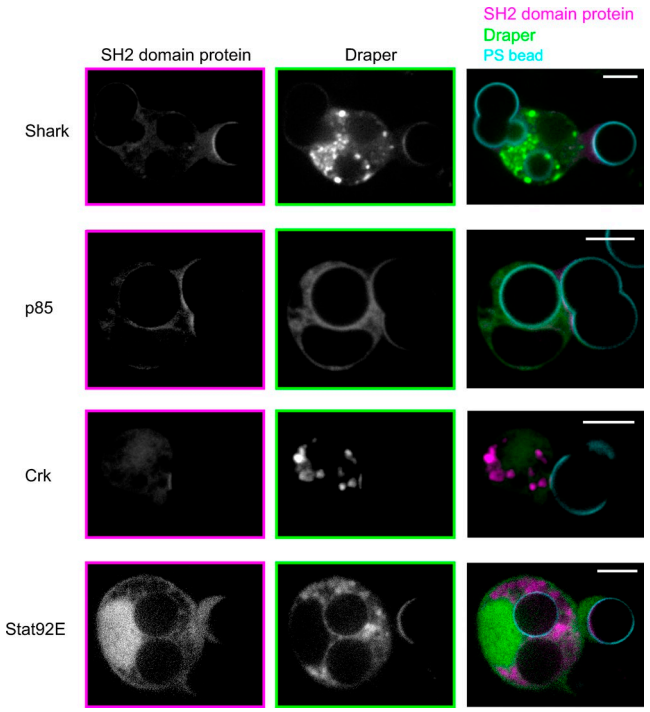

Figure S2. **p85 and Crk are recruited to the synapse with a 10% PS bead (related to Fig. 2).** Draper-mCherry's ability to bring the indicated SH2-GFP proteins to the plasma membrane at the synapse with a 10% PS bead. Shark (three of three synapses examined), p85 (the PI3K activating subunit; three of four synapses examined), and Crk (three of four synapses) were recruited to Draper-mCherry at the synapse, while Stat92E was not recruited (zero of six synapses). Bars, 5 µm.

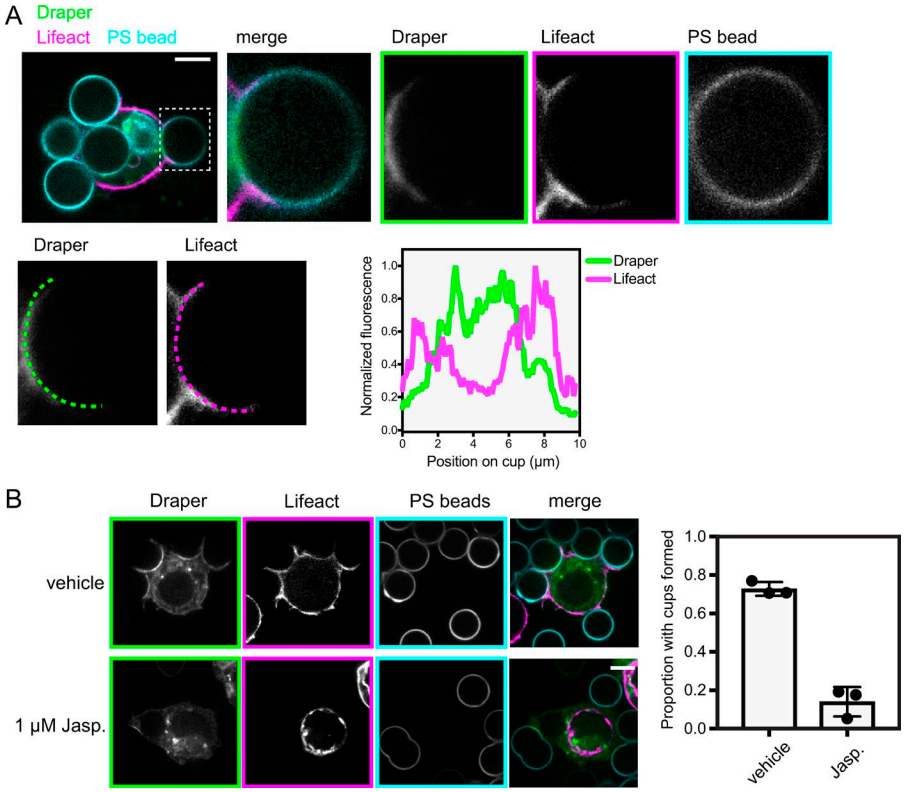

Figure S3. **Characterization of F-actin depletion during engulfment (related to Fig. 2). (A)** Top: F-actin as measured using a LifeAct-EGFP reporter is reduced at sites of Draper-mCherry accumulation at the interface between the bead and target. Localization of Draper-mCherry and LifeAct-EGFP was assessed after 15-min cell settling by spinning-disk confocal microscopy. Depletion of LifeAct-EGFP signal was depleted at 15 of 16 synapses examined. Bottom: A 2-pixel linescan of the phagocytic cup was used to measure LifeAct-GFP and Draper-mCherry signal. Green and magenta dashed lines indicate position of linescan along the cup. Fluorescence above background was normalized to the highest value on the linescan. **(B)** Left: S2 cells transfected with Draper-GFP and LifeAct-TagBFP were treated with 1 µM jasplakinolide or the corresponding volume of vehicle (DMSO) and incubated with 10% PS beads. Jasplakinolide-treated cells were defective in phagocytic cup formation. Addition of jasplakinolide resulted in a mislocalized actin cortex, indicating the drug disrupts actin behavior during the 20-min acute treatment. Each channel is scaled equally between vehicle and jasplakinolide panels. Right: Jasplakinolide-treated cells are defective for phagocytic cup formation, an early stage of Draper-dependent engulfment. The proportion of cells with one or more phagocytic cups after a 20-min treatment with 1 µM jasplakinolide or corresponding volume of vehicle (DMSO) and a 15-min incubation with 10% PS beads is plotted. 72% of vehicle-treated cells formed phagocytic cups (n = 54), while 14% of jasplakinolide-treated cells showed the phenotype (n = 62; mean ± SD from three independent biological replicates is plotted for each condition). Bars, 5 µm.

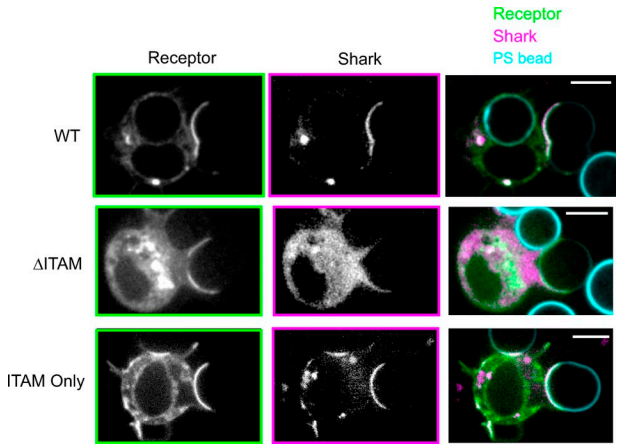

Figure S4. **Draper's ITAM is necessary and sufficient to recruit Shark in cells (related to Fig. 4).** S2 cells cotransfected with Draper, Draper-ΔITAM, or Draper-ITAM only-GFP and Shark-TagBFP were incubated with 10% PS beads labeled with 0.5% atto647-PE. Localization of receptor and Shark-TagBFP was assessed after a 15-min cell settling by spinning-disk confocal microscopy. Images were acquired using the same microscope settings and scaled equally for comparison. Shark-TagBFP was recruited to 11 of 14 Draper, 0 of 15 Draper-ΔITAM, and 10 of 11 Draper-ITAM only-GFP synapses with 10% PS beads examined. Bars, 5 µm.

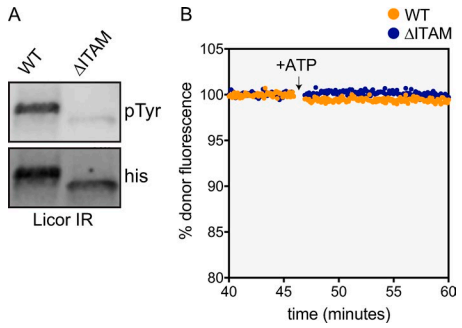

Figure S5. **Biochemical reconstitution of Draper phosphorylation reveals a general triggering mechanism and specific effector recruitment (related to Fig. 5). (A)** To perform on-liposome phosphorylation reactions to assess Draper activation by Lck, 1 µM 10×his-Draper cytoplasmic domain, or 10×his-DraperY934F/Y949F (ΔITAM) receptor tail were ligated to liposomes doped with DGS–Ni-NTA and incubated with 1 nM his_{10}-Lck-Y505F and 1 mM ATP for 30 min. Reactions were quenched with SDS-PAGE buffer containing DTT and 2-Me and boiled for 10 min at 95°C. Samples were run on a 4–20% gradient gel, and pan pTyr (800 nm anti-mouse secondary) was assessed by Western blotting and Li-Cor imaging. Samples were visualized using Li-Cor infrared (IR) imaging. **(B)** The Draper cytosolic domain does not directly bind $p85^{NtSH2}$. A BG505-labeled reporter protein for $p85^{NtSH2}$ was prepared as in Fig. 5 B. The His_{10}-Draper cytosolic domain or His_{10}-DraperY934F/Y949F (ΔITAM) receptor tail was ligated to 0.5% rhodamine-PE liposomes, and ATP-dependent quenching was assessed. A lack of quenching indicates undetectable direct binding between the p85 reporter construct and both Draper and Draper Y934F/Y949F (ΔITAM).

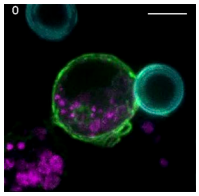

Video 1. **Cellular reconstitution of Draper signaling.** Video of stills shown in Fig. S1 E. An S2 cell cotransfected with Draper-GFP (magenta) and LifeAct-BFP (green) was incubated with 10% PS/0.5% atto647-PE 6.4 µm silica beads (cyan). Video is a maximum projection of a z stack (1 µm between z positions). Z stacks captured by spinning-disk confocal microscopy were recorded every 3 min. Video frame rate is 4 frames per second. Time in minutes. Bar, 5 µm.

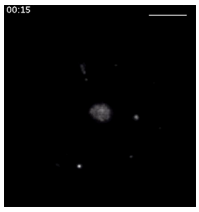

Video 2. **Formation of mobile Draper-GFP microclusters on 10% PS bilayers.** Video of stills shown in Fig. 2 A. An S2 cell transfected with Draper-GFP was allowed to settle on 10% PS SLBs and imaged by TIRF-M. Cell was imaged every 15 s. Draper-GFP forms mobile microclusters that appear at the edge of the spread cell and migrate toward the prominent central synapse of Draper-GFP signal. Video frame rate is 7 frames per second. Time in minutes:seconds. Bar, 5 µm.

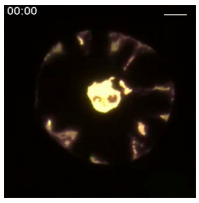

Video 3. **Visualization of signaling microclusters on 10% PS bilayers.** Video of stills shown in Fig. 2 B. An S2 cell cotransfected with Draper-GFP, Shark-TagBFP, and Crk-mCherry was allowed to settle on 10% PS SLBs and imaged by TIRF-M. Cell was imaged every 15 s. Draper-GFP, Shark-TagBFP, and Crk-mCherry colocalize at mobile microclusters that flow toward the central synapse, resulting in a single golden signal. Video frame rate is 3.8 frames per second. Time in minutes:seconds. Bar, 5 µm.

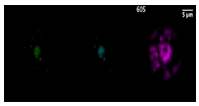

Video 4. **Split channel visualization of Draper, Shark, and F-actin on 10% PS bilayers.** In this split channel video, an S2 cell cotransfected with Draper-GFP (green), Shark-mCherry (cyan), and LifeAct-TagBFP (magenta; Fig. 2 D) was allowed to settle on 10% PS SLBs and imaged by TIRF-M. The cell was imaged every 55 s. Note that Draper-GFP (green), Shark-mCherry (cyan), and LifeAct-TagBFP (magenta) appear at the plasma membrane together, but as clusters mature, the LifeAct reporter segregates from microclusters that contain both Draper and Shark. A prominent F-actin hole is visible later in the video, where the central synapse of Draper-GFP (green)/Shark-mCherry (cyan) signal appears to exclude F-actin as visualized by LifeAct-TagBFP (magenta). Video frame rate is 4 frames per second. Time in seconds.

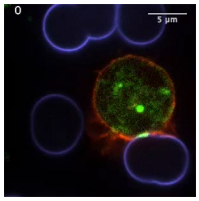

Video 5. **Visualization of FKBP-bead engulfment by a chimeric FRB-Draper receptor.** An S2 cell, cotransfected with FRB-EXT-Draper-INT-mCherry (green) and LifeAct-EGFP (orange), was incubated with 2% DGS-Ni-NTA/0.5% atto390-PE 6.46-µm silica beads incubated with 10 nM His_{10}-FKBP, washed, and resuspended before imaging. FKBP beads were incubated with cotransfected S2 cells in the presence of 1 µM rapamycin, allowed to settle in the imaging chamber for 5 min, and visualized at 5-min intervals by spinning-disk confocal microscopy. Engulfment of an FKBP bead from recognition to internalization is visible at left of this video. Video frame rate is 2.4 frames per second. Time in minutes.

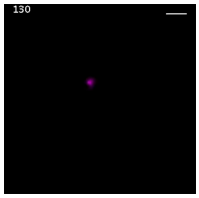

Video 6. **Visualization of FRB-EXT-Draper-INT and LifeAct in an FKBP SLB.** An S2 cell cotransfected with FRB-EXT-Draper-INT-mCherry (green) and LifeAct-EGFP (magenta) was allowed to settle on an SLB adsorbed with His_{10}-FKBP. Imaging was performed in the presence of 1 µM rapamycin, and frames were captured at 65-s intervals. Video frame rate is 5 frames per second. Time in seconds. Bar, 5 µm.

Table S1. **Full supplier and catalog information for materials used in this study**

Reagent	Supplier	Catalog number
Antibodies		
Anti-pTyr mouse; PY20	Santa Cruz Biotechnology	PY20
Anti-Draper 8A1	DSHB/University of Iowa (Iowa City, IA)	8A1
Anti-mouse IgG (H+L) conjugated to Alexa Fluor 647	Thermo Fisher Scientific	A-21236
His-probe antibody rabbit (G-18)	Santa Cruz Biotechnology	G-18
Anti-rabbit IgG (H+L) conjugated to Alexa Fluor 680 (used with 700 nm Li-Cor channel)	Thermo Fisher Scientific	A-21109
IRDye 800CW goat anti-mouse IgG (H+L) antibody (used with 800 nm Li-Cor channel)	Li-Cor	925-32210
Bacterial and virus strains		
Plasmid propagation: Top10 *E. coli*	Invitrogen	C404010
Protein expression: BL-21 DE3 RIPL	Agilent	230280
Chemicals, peptides, and recombinant proteins		
DMSO, tissue culture grade (for cell freezing and vehicle control)	Sigma-Aldrich	D2650
Copper (II) sulfate pentahydrate	Sigma-Aldrich	7758-99-9
Actinomycin D	Sigma-Aldrich	50-76-0
15 ml falcon tubes (CellStar)	Greiner	188 271
1.7 ml Eppendorf tubes	Olympus	24-282
POPC lipid in chloroform	Avanti	850457C
Ni^{2+}-DGS-NTA lipid in chloroform	Avanti	790404C
PEG5000-PE lipid in chloroform	Avanti	880230C
DOPS lipid in chloroform	Avanti	840035C
Atto390-DOPE	ATTO-TEC GmbH	AD 390-161
Atto647-DOPE	ATTO-TECH GmbH	AD 647-161
Rhodamine-PE	Avanti	810150C
Paraformaldehyde	Electron Microscopy Sciences	15712
Triton X-100	Sigma-Aldrich	T8787
BSA	Sigma-Aldrich	A4737
Hellmanex III	Sigma-Aldrich	Z805939
5 N sodium hydroxide	Thermo Fisher Scientific	SS256-500
Rapamycin	Sigma-Aldrich	R0395
Formic acid (0.1% vol/vol), mass spectrometry grade	Thermo Fisher Scientific	LS118-1
Trypsin gold, mass spectrometry grade	Promega	V5280
Iodoacetamide	Sigma-Aldrich	I6125
BSA	Sigma-Aldrich	A7906
PreScission protease	GE Healthcare	27-0843-01
SNAP-Cell 505-Star	NEB	S9103S
Commercial assays		
MycoAlert mycoplasma detection kit	Lonza	LT07-318
MycoAlert mycoplasma control set	Lonza	LT07-518
TransIT-Insect	Mirus	MIR 6100
APC Annexin V	BioLegend	640941
Jasplakinolide	Thermo Fisher Scientific	J7473
Cell line		
Drosophila S2U cells	R.D. Vale lab	FlyBase: FBtc9000006

Reagent	Supplier	Catalog number
Oligonucleotides		
See Table S2, Oligonucleotides tab		
Recombinant DNA		
See Table S2, Constructs tab		
Software and algorithms		
GraphPad Prism	GraphPad Software	6.0
Adobe Photoshop	Adobe	CS6
µManager	µManager/Open Imaging	1.4 (updated using nightly builds)
Fiji (ImageJ)	Fiji.sc	2.0 (updated)
Other		
Schneider's cell culture media	Gibco	21720
FBS, heat inactivated	Atlanta	S11150H
Antibiotic/antimycotic	Gibco	15240062
T75 nonvented tissue culture flask	Corning	430720
T25 nonvented tissue culture flask	Corning	430168
Externally threaded cryovials for freezing cells, 2 ml	Corning	430659
Costar tissue culture–treated 6-well plates	Corning	CLS3516
Polystyrene round-bottom tubes (5 ml) for transfection	Falcon	352058
MatriCal Imaging Plates	Brooks	MGB096-1-2-LG-L
Disposable glass culture tubes (lipid mixes)	Thermo Fisher Scientific	14-961-26
Hamilton syringes (gas tight)	Thermo Fisher Scientific	8 1100
Tissue culture–grade PBS	Gibco	20012050
Drierite	Thermo Fisher Scientific	AC219095000
Bath sonicator to make SUVs	Diagenode	Pico
Extruder for liposome preparation	Avanti	610023
Silica beads for engulfment assay	Bangs Labs	SS06N
Ni-NTA agarose (regenerated)	QIAGEN	30210
Glutathione Sepharose (regenerated)	GE Healthcare	17527901
Superdex 200 10/30 GL column	GE Healthcare	17517501
PD Minitrap G-25 column (remove excess BG505 dye)	GE Healthcare	28-9180-07

Provided online is one table in Excel. Table S2 shows detailed information for all recombinant DNA materials.